Measurement of the Lateral Diffusion of Dipalmitoylphosphatidylcholine Adsorbed on Silica Beads in the Absence and Presence of Melittin: A ^{31}P Two-Dimensional Exchange Solid-State NMR Study

Frédéric Picard,* Marie-Josée Paquet,* Érick J. Dufourc,# and Michèle Auger*
*Département de Chimie, Centre de Recherche en Sciences et Ingénierie des Macromolécules, Université Laval, Québec,
Québec G1K 7P4, Canada, and #Centre de Recherche Paul Pascal, CNRS, 33600 Pessac, France

ABSTRACT ^{31}P two-dimensional exchange solid-state NMR spectroscopy was used to measure the lateral diffusion, D_L, in the fluid phase of dipalmitoylphosphatidylcholine (DPPC) in the presence and absence of melittin. The use of a spherical solid support with a radius of 320 ± 20 nm, on which lipids and peptides are adsorbed together, and a novel way of analyzing the two-dimensional exchange patterns afforded a narrow distribution of D_L centered at a value of $(8.8 \pm 0.5) \times 10^{-8}$ cm^2/s for the pure lipid system and a large distribution of D_L spanning 1×10^{-8} to 10×10^{-8} cm^2/s for the lipids in the presence of melittin. In addition, the determination of D_L for nonsupported DPPC multilamellar vesicles (MLVs) suggests that the support does not slow down the lipid diffusion and that the radii of the bilayers vary from 300 to 800 nm. Finally, the DPPC-melittin complex is stabilized at the surface of the silica beads in the gel phase, opening the way to further study of the interaction between melittin and DPPC.

INTRODUCTION

In the well-established fluid mosaic model of membranes, the lipids are organized in the form of a bilayer supporting extrinsic and intrinsic proteins (Singer and Nicolson, 1972). In this model, the lipid bilayer can be considered a two-dimensional fluid in which lipids and proteins are free to diffuse laterally. This lateral diffusion of lipids and proteins is a property that directly reflects the fluidity of the biological membrane. Therefore, many techniques have been used, since the elaboration of the fluid mosaic model, to precisely determine the lateral diffusion constant (Vaz et al., 1984; Tocanne et al., 1989). Among the most widely used techniques is fluorescence recovery after photobleaching (FRAP) (Tocanne et al., 1989), quasielastic neutron scattering (QENS) (Köchy and Bayerl, 1993), and NMR spectroscopy (Fenske et al., 1991; Heaton et al., 1996; Lindblom and Orädd, 1996; Karakatsanis and Bayerl, 1996).

NMR spectroscopy is a very useful technique for the study of biological and model membranes (Griffin, 1981; Bloom and Bayerl, 1995). In the last 20 years, this technique and, particularly, ^{2}H (Davis, 1983, 1991; Seelig, 1977) and ^{31}P (Seelig, 1978; Smith and Ekiel, 1984) NMR spectroscopies have provided a lot of information about the structure and dynamics of the lipid bilayer, as well as on the interaction between lipids and proteins. A very important advantage of the NMR technique is that it can provide information about the dynamics on a large time scale, from 10^{-10} to 10^0 s. Using ^{2}H NMR spectroscopy, Bloom and Sternin (1987) have shown that the transverse relaxation time measured by

the CPMG (Carr-Purcell-Meiboon-Gill) pulse sequence (Carr and Purcell, 1954; Meiboom and Gill, 1958) can be very sensitive to slow motions such as the lateral diffusion of lipids. Under certain conditions, when there is a predominance of lateral diffusion on other slow motions (Dolainsky et al., 1993), this method can give very precise values of the lateral diffusion constant (Köchy and Bayerl, 1993). Furthermore, by the use of pulsed (Lindblom and Orädd, 1996) or static gradients (Karakatsanis and Bayerl, 1996), it is possible to measure very precisely the diffusion of lipids along this particular magnetic field direction.

The lateral diffusion of lipids can also be studied by two-dimensional NMR (Jeener et al., 1979; Auger et al., 1991; Fenske and Jarrell, 1991) and uses the fact that in solid-state NMR, the chemical shielding or the electric quadrupolar tensors show an orientational dependence in the static magnetic field. Therefore, it is possible to observe correlation peaks in a two-dimensional spectrum map representing an orientational exchange originating from the diffusion of lipids over the curved membrane surface. Jarrell and co-workers have shown that slow motions in lipids can be observed by 2D ^{2}H NMR spectroscopy (Auger and Jarrell, 1990; Auger et al., 1991) and have measured the diffusion constant of different phospholipids by ^{31}P NMR spectroscopy (Fenske and Jarrell, 1991; Fenske et al., 1991; Fenske and Cullis, 1992). On the other hand, Macquaire and Bloom (1995) have developed a mathematical model showing that lateral diffusion is the main slow motion on highly curved vesicles, and Dolainsky et al. (1995) have used this mathematical model to determine the lateral diffusion constant of phospholipids on spherical supported vesicles by 2D ^{2}H NMR spectroscopy.

A method for determining the isotropic rotational diffusion from 2D NMR exchange spectra has been developed by Schmidt-Rohr and Spiess (1994) and used by Barrall et al. (1995) on polymers. This method is close to the intuitive

method elaborated by Fenske et al. (1991) and is based on the calculation of the time-dependent orientational autocorrelation function of order 2, $C_2(t_m)$. This function decays exponentially with time, and the decay constant is directly related to the rotational diffusion constant. If the radius of the system studied is known, the lateral diffusion constant is easily determined.

All of these methods require the precise value of the phospholipid vesicle radius. However, in all cases, it was a rough approximation, because of the radius polydispersity and the multilamellar nature of the model membrane used. Heaton et al. (1996) have recently shown by ^{31}P NMR that in a lipid dispersion, the radius distribution is extremely broad, spanning more than two orders of magnitude in the case of pure DMPC, and therefore questioned the accuracy of the above finding. As a consequence, the determination of the lateral diffusion of lipids by 2D NMR relies on the control of the radius of the lipid vesicles.

Supported bilayers as model membranes are now widely used. In ATR-FTIR (attenuated total reflectance-Fourier transform infrared) spectroscopy, lipid bilayers deposited on a germanium crystal are used to determine lipid orientation (Fringeli and Günthard, 1981; Désormeaux et al., 1992; Nabet et al., 1994). On the other hand, lipids deposited on silica plates are used to measure lipid diffusion by QENS (Johnson et al., 1991; König et al., 1992). Bayerl and Bloom (1990) have developed a new model of supported lipid membranes. In this spherical model, lipids are deposited on silica beads. This model is particularly useful for the study of lipids in high-field NMR, where the vesicles may be deformed by the magnetic field (Brumm et al., 1992; Pott and Dufourc, 1995). The use of spherical supported vesicles (SSVs) also makes it possible to control the radius of the vesicles and to obtain only one bilayer per bead (Bayerl and Bloom, 1990). In addition, Naumann et al. (1992) have shown that the bilayer is not disrupted by variation in the temperature below and above the lipid phase transition temperature. In the past this model was widely used and gave rise to many interesting results on lipid-protein interactions (Reinl and Bayerl, 1993), ultraslow motions in lipid bilayers (Dolainsky et al., 1993), and lateral diffusion of lipids (Köchy and Bayerl, 1993; Dolainsky et al., 1995).

In the present study, we have used the above model to determine the lateral diffusion constant of dipalmitoylphosphatidylcholine (DPPC) deposited on silica beads by a 2D ^{31}P NMR approach similar to the one used by Barrall et al. (1995) for the determination of rotational diffusion in polymers. One of the goals of our study is to determine whether the beads alter the diffusion of lipids and therefore to verify whether the SSV model is a good system for the study of lateral diffusion of lipids.

On the other hand, the effect of proteins on membrane fluidity is of considerable interest (Vaz et al., 1984), and it is therefore very important to measure the lateral diffusion of the proteins themselves and of the lipids in interaction with these proteins. In the present study, we have investigated the effect of melittin on the lateral diffusion of DPPC.

This amphipatic toxin protein extracted from honey bee (*Apis mellifera*) venom is a 26-amino acid α-helical peptide whose main property is to induce membrane lysis. It has been demonstrated that melittin promotes dramatic changes in the structure and dynamics of model and natural membranes (Cornut et al., 1993; Dufourc et al., 1989; Pott and Dufourc, 1995; Pott et al., 1996; for a review see Dempsey, 1990). With model membranes composed of zwitterrionic lipids such as dipalmitoylphosphatidylcholine, melittin forms small discoidal structures (~200 Å radius) below the phase transition temperature of the pure lipid and large unilamellar vesicles (~2500 Å radius) above (Dasseux et al., 1984; Dufourc et al., 1986a; Dufourcq et al., 1986). At the phase transition temperature, a restructuring of the membrane occurs to form large lipid lamellas. This phenomenon is known to be reversible and to be present in natural membranes (Dufourc et al., 1989; Katsu et al., 1988, 1989).

Lipid dynamics in the presence of melittin has already been investigated. In particular, local membrane ordering is markedly reduced by melittin for fluid phase temperatures far from the main transition. On the other hand, fast lipid motions are unaffected by the toxin (Dufourc et al., 1986b). Our goal here is to study the effect of melittin on the lipid slow motions such as the lateral diffusion. We have also characterized the system by determining the amount of DPPC and melittin adsorbed on the silica beads. This was done by FTIR, because of the high precision and sensitivity of this technique and because of the possibility of studying in a quantitative way both melittin and DPPC by a judicious choice of the studied IR bands.

THEORY

Time-dependent orientational autocorrelation function

This section will introduce some helpful concepts for the determination of the lateral diffusion constant from the experimental spectra. Note that the following theoretical treatment is presented only to allow the noninitiated reader to understand the origin of the concepts given in the text. A deeper theoretical treatment is given in Chapter 9 of Schmidt-Rohr and Spiess (1994).

When a system has an axial symmetry like the one found in phospholipid membranes, it is possible to describe the NMR chemical shifts by the equation

$$\omega(\theta) = \delta[(3\cos^2\theta - 1)/2] = \delta P_2(\cos\theta) \qquad (1)$$

where θ is the angle formed by the principal axis of chemical shift tensor and the static magnetic field. To simplify this equation, the chemical shift anisotropy parameter, δ, is expressed in frequency units, and the isotropic chemical shift is defined as being equal to 0. Equation 1 shows that the chemical shift angular dependence is, in fact, a second-order Legendre polynomial, $P_2(\cos\theta)$.

In two-dimensional exchange NMR spectroscopy, correlations between two angular-dependent frequencies are

measured. A function that measures the correlation of another function at a time 1 and at a time 2 for a stochastic process such as the lateral diffusion or other Brownian motions (Abragam, 1961) can be defined. In our case, these functions 1 and 2 are, in fact, the initial and final frequencies of the system. Thus we can define the time-dependent autocorrelation function, $C_f(t)$:

$$C_f(t_m) = \langle \omega_1 \omega_2 \rangle / \langle \omega_1^2 \rangle \tag{2}$$

where $\omega_1 = \omega(\theta_1)$, $\omega_2 = \omega(\theta_2)$, $\theta_1 = \theta(0)$, and $\theta_2 = \theta(t_m)$. The mixing time, t_m, is defined in the Experimental section. It is possible as well to express this reorientational stochastic process in terms of a joint probability density. This can be a probability density between two angles, or between two frequencies. When expressed for two frequencies, the upper part of Eq. 2 becomes

$$\langle \omega_1 \omega_2 \rangle = \int \int \omega_1 \omega_2 S(\omega_1, \omega_2; t_m) d\omega_1 \, d\omega_2 \tag{3}$$

In fact, this probability density, $S(\omega_1, \omega_2; t_m)$, is the two-dimensional spectral density obtained with the 2D exchange pulse sequence. A frequent way of defining the correlation function is with the Legendre formalism. Because our system is correctly described by a second-order Legendre polynomial, the autocorrelation function will be of order 2. Note that superior order autocorrelation functions can be calculated from 2D spectra (Spiess, 1991), but these notions will not be used here. Thus the function written in Eq. 2 can be rewritten as

$$C_2(t_m) = \frac{5}{\delta^2} \int \int \omega_1 \omega_2 S(\omega_1, \omega_2; t_m) d\omega_1 \, d\omega_2 \tag{4}$$

with these two conditions:

$$\langle \omega_1^2 \rangle = \langle \delta^2 P_2^2(\cos\theta_1) \rangle = \delta^2/5 \tag{5}$$

$$\int \int S(\omega_1, \omega_2; t_m) d\omega_1 \, d\omega_2 = 1 \tag{6}$$

Because both δ and ω are expressed in frequency units, the C_2 values are dimensionless.

Determination of correlation times

The autocorrelation function, $C_2(t_m)$, introduced in the last section will decay exponentially with the mixing time. The decay factor is the rotational correlation time, t_d:

$$C_2(t_m) = \exp\left(-\frac{t_m}{t_d}\right) \tag{7}$$

This correlation time is linked to the vesicle radius, r, and to the lateral diffusion constant, D_L, via the following equation (Abragam, 1961), assuming that the tumbling of the

vesicles is neglected (see next section):

$$D_L = \frac{r^2}{l(l+1)t_d} \overset{l=2}{\Rightarrow} \frac{r^2}{6t_d} \tag{8}$$

Stochastic processes with a single correlation time, however, will rarely be found. We can imagine rather a distribution of correlation times, $g(t_d)$. In such cases, Eq. 7 becomes

$$C_2(t_m) = \int g(t_d)\exp\left(-\frac{t_m}{t_d}\right)dt_d \tag{9}$$

with the condition

$$\int g(t_d)dt_d = 1 \tag{10}$$

This distribution of correlation times can have different shapes. A generally accepted shape is the log-Gaussian shape (Schaefer and Spiess, 1992; Schmidt-Rohr and Spiess, 1994):

$$g(t_d) = \frac{1}{t_d\sigma_{\ln}\sqrt{2\pi}} \exp\{-[\ln(t_d/t_d^\circ)]^2/\sigma_{\ln}^2\} \tag{11}$$

where $\ln(t_d^\circ)$ is the center of gravity of the distribution in the $\ln(t_d)$ domain and $\sigma_{\ln}$ is approximately the width in decades. This distribution of correlation times can originate either from a distribution of vesicle radii or from a distribution of lateral diffusion constants, as suggested by Eq. 8. When an experiment is performed with a fixed radius, it can be assumed that the distribution of t_d comes solely from a distribution of D_L. A distribution of D_L can be calculated from $g(t_d)$ with the equation

$$g(D_L)dD_L = g(t_d)dt_d \Rightarrow g(D_L) = g(t_d)\frac{t_d}{D_L} \tag{12}$$

On the other hand, if the distribution of t_d comes solely from a distribution of radii, we can calculate this distribution with the equation

$$g(r)dr = g(t_d)dt_d \Rightarrow g(r) = g(t_d)\frac{2t_d}{r} \tag{13}$$

Finally, it is always possible to calculate a value of t_d without any assumption about the shape of the distribution by using the Kohlraush-Williams-Watts (KWW) equation (Williams and Watts, 1970):

$$C_2(t_m) = \exp\left(-\left[\frac{t_m}{t_d}\right]^\beta\right) \tag{14}$$

where β varies between 0 and 1.

Normalized root mean square deviation method

To obtain the values of t_d, a method to fit the experimental data with the previously described distribution function had to be developed. In this case, a normalized root mean square (RMS) deviation method is used. The RMS is defined as

$$\text{RMS}(\%) = \frac{\sqrt{\sum (C_2^{\text{exp}} - C_2^{\text{fit}})^2}}{\sqrt{\sum (C_2^{\text{exp}})^2}} \times 100 \qquad (15)$$

The fit is therefore modified until the minimum RMS is reached. The value of the RMS in percent is related to the mean relative error for each data point of the curve. Finally, the fact that this function is normalized will help the comparison between fits obtained for different experiments.

Tumbling versus lateral diffusion

Equation 9 shows that the rotational correlation time can be related directly to the lateral diffusion constant. In fact, the correlation time measured experimentally can be due to several phenomena, which result in an orientational change of the chemical shift tensor principal axis relative to the static magnetic field. However, two major processes have to be considered, lateral diffusion and tumbling of the vesicles. The correlation time measured experimentally, t_e, is related to the correlation time due to diffusion, t_d, and the correlation time due to tumbling, t_t:

$$1/t_e = 1/t_d + 1/t_t \qquad (16)$$

Therefore, tumbling can be neglected only if $1/t_d \gg 1/t_t$. The correlation time due to tumbling is defined as

$$t_t = 4\pi\eta r^3/3kT \qquad (17)$$

where η is the solvent viscosity, k is the Boltzmann constant, T is the temperature, and r is the radius of the vesicle. If we consider the viscosity of water at 323 K (550 μPa · s) and a radius of 320 nm, we find a tumbling correlation time of ~20 ms. However, the viscosity of lipid samples is most likely much greater than the viscosity of pure water, resulting in an increase in the tumbling correlation time. In addition, a lipid sample deposited on glass beads is far from an aqueous solution. In this case, the lipid-bead complex will precipitate in the bottom of the tube, because of the high density of the beads (2.5 g/cm^3). This will result in a system to which Eq. 17 is not directly applicable and for which tumbling will not be favored. Therefore, for experimental correlation times on the order of a few milliseconds, the effect of tumbling can be safely neglected.

EXPERIMENTAL

Materials

Dipalmitoylphosphatidylcholine (DPPC) was obtained from Avanti Polar Lipids (Alabaster, AL) and used without further purification. Melittin used for the NMR experiments was obtained from Biowhittaker (SERVA) (Fontenay sous Bois, France) and used without further purification,

whereas melittin used for the FTIR experiments was obtained from Fluka (Ronkonkoma, NY) and used without further purification. The beads ($r = 320 \pm 20$ nm), consisting of silica of the highest purity, were generously provided by Dr. Thomas M. Bayerl. Beads were recycled between experiments. For experiments with the pure lipid, the beads were washed six times with methanol. When melittin was used, the beads were washed three more times with an acetonitrile-aqueous solution (55/45, v/v) (1 M KClO$_4$, pH 2.5).

Sample preparation

NMR experiments

The buffer used for the NMR samples was prepared by mixing 100 mM NaCl, 2 mM EDTA, and 20 mM Tris-HCl at a pH of 7.5. The pH was measured with a microelectrode (Microelectrodes, Londonderry, NH) and adjusted with diluted NaOH or HCl. Melittin was dissolved in a buffer at a concentration of 10% (42 mM). Aqueous dispersions of DPPC were prepared by mixing the appropriate amount of solid in the buffer solution. Samples containing 15% by weight of lipids were then heated at ~65°C for 10 min, stirred on a vortex mixer, and cooled down at 0°C for 10 min. This cycle was repeated at least five times to obtain multilamellar vesicles. According to Bayerl and Bloom (1990), the spherical supported vesicles (SSVs) of pure DPPC were prepared by condensing small unilamellar vesicles (SUVs) on the silica beads. The SUVs were prepared by sonication with an Ultrasonic titanium rod sonicator (200 W output power, pulse mode 40% duty cycle; Heat System-Ultrasonics, Plainview, NY). The use of the pulse mode and an external water bath kept the temperature below 50°C during sonication. The SUVs were then heated at 60°C for 2 min and mixed with dry beads with vigorous vortexing. The sample was then centrifuged and the supernatant was discarded. The coated glass beads in the pellets were redispersed in a fourfold excess volume of buffer, vortexed, and centrifuged again to remove excess lipids. This washing step was repeated six times. Three times the amount of DPPC required to cover the total glass surface with one continuous bilayer was chosen to ensure that all of the beads were covered. It was assumed in this calculation that the headgroup area of DPPC is 71.2 Å^2 (Lis et al., 1982) and that the beads have a density of 2.5 g/cm^3. The SSVs of the DPPC:melittin complexes were prepared by mixing the lipid SUVs and a melittin solution to obtain a 20:1 lipid-to-protein molar ratio. In these proportions, melittin and DPPC form small discoidal assemblies below the phase transition temperature of the pure lipid (Dufourc et al., 1986a; Dufourcq et al., 1986). These complexes were then added to the dry silica beads. The next steps are the same as for pure DPPC. A twofold excess of water is kept during the NMR experiments.

FTIR spectroscopy experiments

The FTIR buffer (100 mM NaCl, 2 mM EDTA, and 20 mM Tris-HCl) was first prepared in D$_2$O at a pD of 7.9 and dried by lyophilization. The buffer was then rehydrated with D$_2$O and the pD was readjusted at 7.9 with diluted NaOD and DCl to avoid interference from H$_2$O in the infrared spectra. The silica beads were also hydrated with D$_2$O and dried by lyophilization to decrease the exchange of proton from silica to the buffer solution. All of the other steps were identical to the sample preparation described for the NMR experiments. The standards for the dosage were prepared by the dilution of a DPPC SUV solution (15% by weight) to obtain seven solutions with concentrations between 0.5% and 15% and by the dilution of a melittin solution (2% by weight (8.4 mM)) to obtain seven solutions with concentrations between 0.05 and 1.5% (0.2–6.3 mM).

NMR experiments

For the experiments on spherical supported vesicles, the ^{31}P NMR spectra were acquired at 121.5 MHz on a Bruker ARX-300 implemented for

high-power solid-state spectroscopy. Experiments were carried out with a broadband/^{1}H dual-frequency 10-mm probehead under conditions of gated WALTZ proton decoupling. One-dimensional spectra (2048 scans) were recorded using a Hahn echo pulse sequence with WALTZ decoupling during acquisition (Rance and Byrd, 1983). The ^{31}P $\pi/2$ pulse length was ~8 μs, the pulse spacing was 40 μs, and the recycle time was 6 s. For the experiments on multilamellar vesicles, the ^{31}P NMR spectra were acquired at 121.5 MHz on a Bruker ASX-300 (Bruker Spectrospin, Milton, ON, Canada) operating at a ^{1}H frequency of 300.00 MHz. Experiments were carried out with a broadband/^{1}H dual-frequency 4-mm probehead under conditions of CW proton decoupling. The ^{31}P $\pi/2$ pulse length was ~5 μs, and the recycle time was 4 s.

The two-dimensional spectra were recorded using the NOESY pulse sequence with TPPI to give quadrature detection in both dimensions (Bodenhausen et al., 1984):

$$90_x^\circ - t_1 - 90_x^\circ - t_m - 90_x^\circ - t_2 \qquad (18)$$

where t_1 is the evolution time, t_m is the mixing time, and t_2 is the detection period. Decoupling was gated on during t_1 and t_2. The t_m were varied from 50 μs to 600 ms, and the recycle time was set to 4 s. The data sets contained 256 points in the F_2 dimension, zero-filled to 512, and 64 points in the F_1 dimension, zero-filled to 512. Between 256 and 512 scans were recorded for each serial file in a given 2D experiment. For most experiments, the spectral width in both dimensions was 50 kHz. The temperature was controlled within 0.5°C, and the chemical shifts (expressed in ppm) were referenced to external phosphoric acid at 0 ppm.

FTIR experiments

Infrared spectra were recorded on a Nicolet Magna 550 Fourier transform infrared spectrometer equipped with a narrow-band mercury-cadmium-telluride detector and a germanium-coated KBr beam splitter. A total of 250 scans were averaged at 2 cm^{-1} resolution after triangular apodization. Approximately 10 μl of sample was contained between two BaF$_2$ windows separated by a 6-μm Mylar spacer in a homemade transmission cell thermoelectrically regulated at 50°C. DPPC was dosed by analyzing the CH$_2$ antisymmetrical vibrations of the lipid acyl chains at 2920 cm^{-1} after a polynomial baseline correction, and melittin was dosed by analyzing the amide I band at 1640 cm^{-1} after polynomial baseline correction. All experiments were carried out in D$_2$O to eliminate interference from the bending vibration mode of H$_2$O in the amide I region.

RESULTS

The melittin-DPPC-beads system

We first used FTIR spectroscopy to quantify the exact amounts of melittin and DPPC deposited on the silica beads to characterize the system studied. Regression curves with a 98% regression coefficient were obtained in both cases. Even with six washing steps in the experimental protocol, the systems prepared at a lipid/protein molar ratio of 20:1 remained at that ratio throughout the experiment when deposited on the beads. In both the absence and presence of melittin, the total amount of lipids deposited on the beads always corresponds to ~1.5 lipid bilayers per bead. Other FTIR results have also shown that melittin can bind to the beads without the presence of DPPC in the same proportion as they do in the presence of DPPC (data not shown). These results demonstrate that there is no preferential interaction of melittin or DPPC with the beads and hence suggest that

the melittin-DPPC complexes are not perturbed by adsorption to the surface.

The one-dimensional NMR results are in agreement with the above observations. Fig. 1 shows the thermal evolution of a system prepared as previously described to obtain one bilayer per bead. It is already known that a DPPC-melittin complex in the gel phase and at a lipid/protein molar ratio of 20:1 gives rise to a unique isotropic peak around 0 ppm (Dufourc et al., 1986a,b). Fig. 1 *A* shows the spectrum obtained for the system immediately after its preparation in the gel phase. This spectrum does not show an isotropic peak at 0 ppm, indicating that there are no free discs in solution. An isotropic peak appears when the system is cooled down (Fig. 1, *C* and *F*), but only in small proportions, and it disappears with time (Fig. 1 *D*). Apparently, small discoidal complexes appear in solution, when the temperature is cooled down below the phase transition temperature. Perturbation of the lipid organization is often associated with the phase transition. In fact, the headgroup area changes at this transition, and the lipids have to reorganize themselves in a stable structure. In the present case,
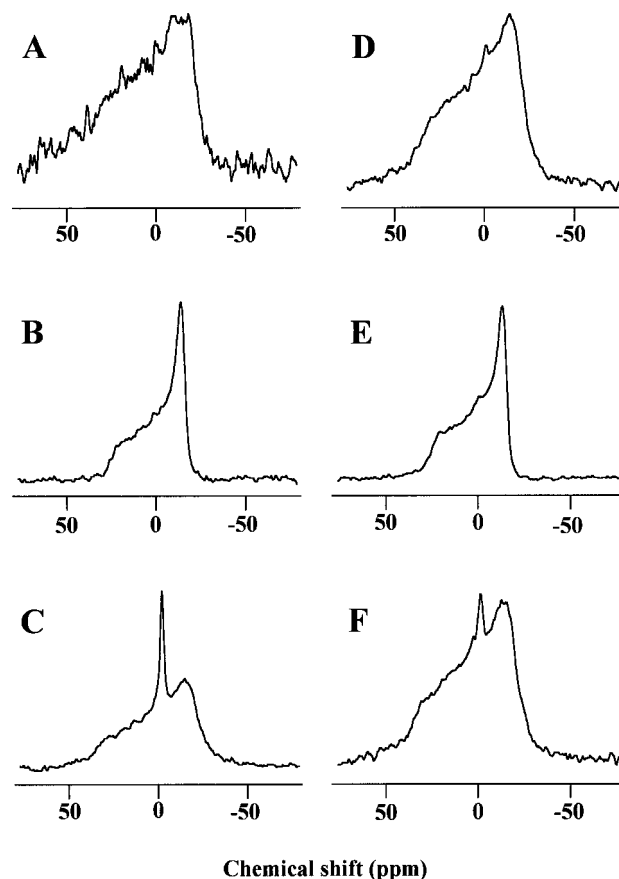

FIGURE 1 Time and temperature dependencies of the ^{31}P NMR spectra for the DPPC-melittin complex at a lipid-to-protein molar ratio of 20:1. Spectra recorded at (*A*) 30°C, 30 min after the washing steps; (*B*) 50°C, after a week at this temperature; (*C*) 30°C, 30 min after the previous spectrum; (*D*) 30°C, after a week at this temperature; (*E*) 50°C, 30 min after the previous spectrum; (*F*) 30°C, immediately after the previous spectrum.

this reorganization seems to create a perturbation that promotes the formation of unstable small discoidal structures. However, the system reaches a new equilibrium with time with all of the melittin and DPPC on the beads. This phenomenon of the disappearance of the small discs with time has already been observed by ^{31}P NMR spectroscopy for melittin-DPPC complexes, but only after many days of incubation below the phase transition temperature (Faucon et al., 1995).

Determination of the diffusion time

In solid-state two-dimensional NMR, cross-intensity appears when there is a change of orientation during t_m. We can conclude in a 90° change when cross-intensity appears between the 0° and 90° orientations. Such cross-intensity will result in a square spectrum, and the time required for this to happen is called the 90° diffusion time, $t_{90°}$, which is very close to the t_d that we wish to determine. An intuitive method for determining $t_{90°}$ consists of finding the 2D spectrum with the shortest t_m that has a L/W (spectrum length/spectrum width) ratio of 1.0. Fenske et al. (1991) have developed a method derived from this principle. Spectra with different t_m around the approximate $t_{90°}$ are acquired, and a graph of L/W versus t_m is drawn. On this graph, the time where the measured value of L/W becomes constant is $t_{90°}$. This method is valid for the lowest contour level of the spectra. For large NMR samples (over ~30 mg of lipids), it is relatively easy to measure the intensity of the low contour levels. However, for smaller samples such as the ones used in the present study (~7 mg of lipids), the spectral noise is maximum in the lower contour levels, and the width and length are therefore more difficult to estimate. Therefore, we have used a more rigorous method where a real t_d is determined instead of $t_{90°}$. This method is described in detail in the Theory section. It is based on a calculation over the whole spectrum, and therefore there is no loss of information, as in the Fenske et al. (1991) method. In addition, it is less sensitive to spectral noise and can be used to analyze spectra with a lower signal-to-noise ratio.

Measurement of the diffusion time of pure DPPC adsorbed on silica beads

The two-dimensional spectra of pure DPPC adsorbed on silica beads are shown in Fig. 2. The lateral diffusion is already present at a mixing time of 500 μs, seems to be very advanced at 3 ms, and is complete, at least for the lowest contour levels, at $t_m = 5$ ms, although there is an evolution of the medium and highest contour levels up to a mixing time of 20 ms. These observations confirm the assumption made earlier that the L/W ratio varies with the contour level used for the calculation. Therefore, Eq. 4 was used to determine the autocorrelation function (C_2) of the different 2D spectra. The variation of C_2 as a function of mixing time
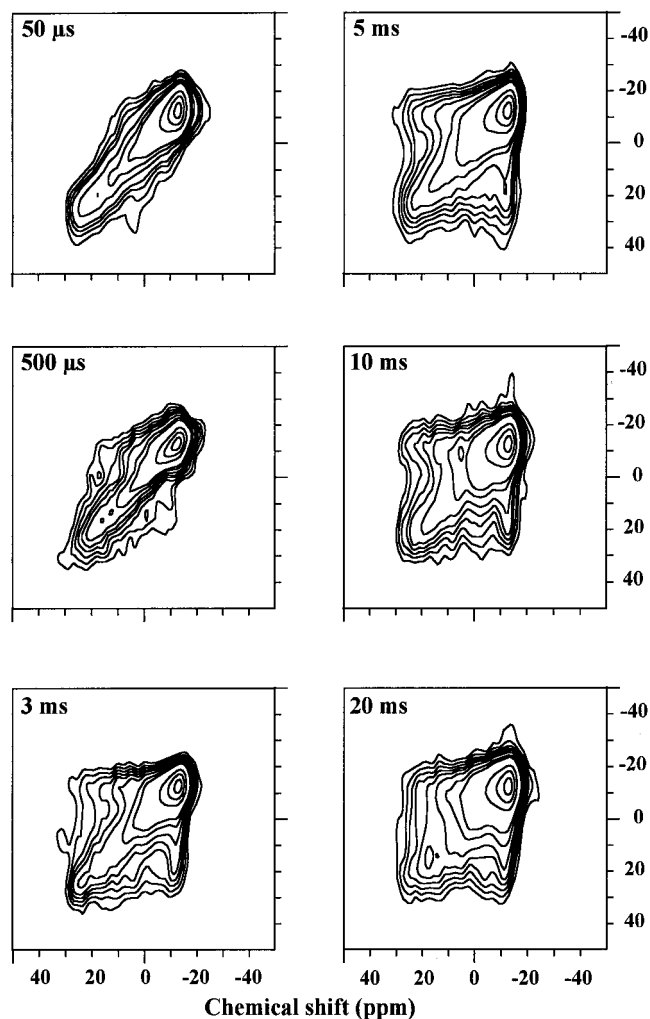

FIGURE 2 2D ^{31}P NMR experimental spectra of pure DPPC SSV at 50°C for different t_m.

is plotted in Fig. 5 A. We can readily see that this function decays exponentially. The fit represented in this figure is a single-exponential function, and Table 1 summarizes the

TABLE 1 t_d values obtained from different distribution functions

	DPPC-beads $r = 320$ nm	DPPC-MLV $r = 500$ nm	DPPC-melittin-beads $r = 320$ nm
Log-Gaussian distribution			
t_d (ms)	2.0	5.0	3.3
D_L (cm²/s)		8.3×10^{-8}	5.1×10^{-8}
σ_{ln}	0.0	0.5	0.9
RMS (%)	2.1	0.65	1.1
KWW function			
t_d (ms)	2.0	5.0	3.4
β	1.0	0.9	0.7
RMS (%)	2.1	0.58	1.1
No distribution			
t_d (ms)	2.0	5.2	3.3
D_L (cm²/s)	8.8×10^{-8}		
RMS (%)	2.1	0.84	4.6

different possible curves that can be used to fit the experimental data. The value of the correlation time found without the use of a distribution is 2.0 ± 0.2 ms. A regression of the KWW type (Eq. 14) gives a β value of 1, which confirms that there is probably no distribution of diffusion constants. These two fits give a RMS value of 2.1%, which is relatively good, considering the dispersion of the experimental data points. With this t_d value and with the knowledge of the mean vesicle radius (320 nm), we can calculate a lateral diffusion constant of $(8.8 \pm 0.5) \times 10^{-8}$ cm^2/s. The fact that there is no distribution of correlation times measurable by our technique shows that the distribution of bead radii is probably included in the experimental error. This result also shows that within experimental error, all lipids undergo diffusion with the same diffusion constant. Therefore, if a distribution of t_d is found in a multilamellar system of DPPC, this will be due most likely to a distribution of radii and not to a distribution of D_L.

Effect of melittin on the lateral diffusion time of DPPC adsorbed on silica beads

Two-dimensional spectra of the DPPC-melittin complex (at a lipid/protein molar ratio of 20:1) are shown in Fig. 3. As in the pure DPPC case, the lateral diffusion is easily seen on the different spectra. This lateral diffusion is present on the spectra with mixing times of 1, 3, and 5 ms and seems to be complete for all intensity levels at 10 ms. The spectra are of greater quality because the lower contour levels are well identified, but are very similar to the spectra obtained for pure DPPC in the presence of lateral diffusion. On the other hand, when the autocorrelation time functions were calculated for all spectra (Fig. 5 B), we can easily see the difference between the two systems. The curve used to fit the experimental data obtained in the presence of melittin is a log-Gaussian distribution that gives a low RMS, indicating that this function is able to correctly fit the experimental data. In Table 1, all of the tested fitting functions are reported. The KWW function gives the same RMS value, but this function does not give any information about the shape of the distribution. The use of a single exponential function gives a really high RMS value, which confirms the presence of a broad distribution of t_d. A Gaussian distribution was also tested, but the result obtained had no physical significance, because this distribution function gave a large population of t_d values at mixing times close to 0 ms and therefore at infinite values of D_L. We can also see in Table 1 that all of the values of t_d found with all of the fitting functions are greater than in the pure DPPC-bead case. This corresponds to a slowing down of the lipids, as was expected. Using the width of the log-Gaussian distribution ($\sim$1 decade), values of t_d spanning from 1.3 to 9.5 ms were found. The corresponding D_L distribution (calculated with a fixed radius of 320 nm) gives values ranging from 2×10^{-8} to 13×10^{-8} cm^2/s, with a mean D_L value of 4.9×10^{-8}
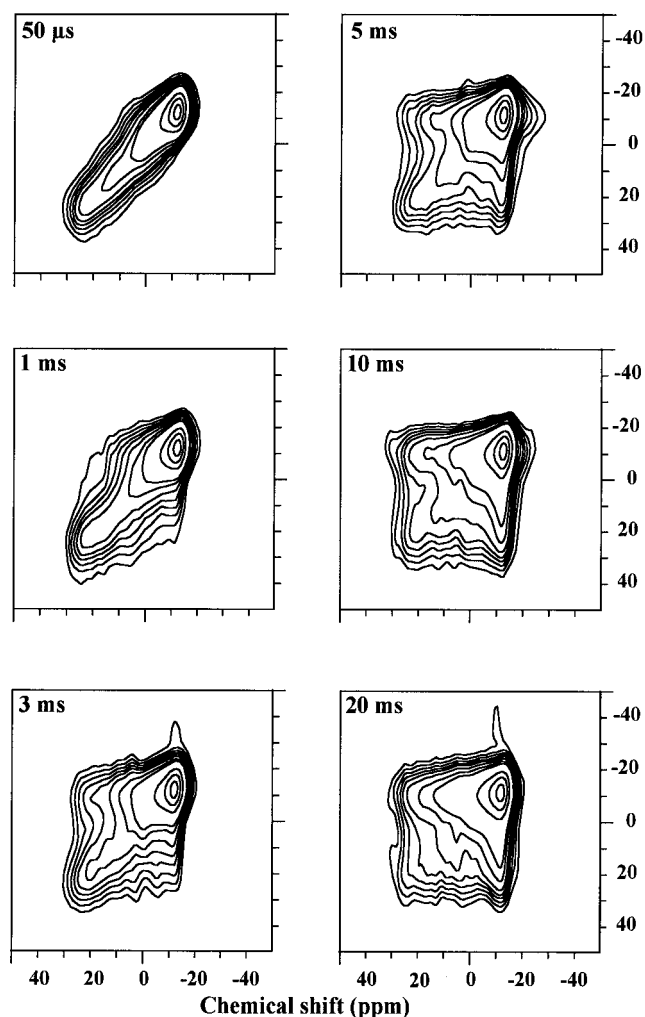

FIGURE 3   2D ^{31}P NMR experimental spectra of SSV of the melittin-DPPC complex (lipid-to-protein molar ratio of 20:1) at 50°C for different t_m.

cm^2/s. Representations of these distributions are shown in Fig. 6, A and B.

Effect of the beads on the lateral diffusion time of DPPC

Lateral diffusion measurements were also performed on a nonsupported DPPC multilamellar system to determine whether the beads are slowing down the lipid diffusion. This could also allow the characterization of the radius distribution for this type of sample. The experimental spectra are presented in Fig. 4, and the calculated autocorrelation time function curve for the DPPC MLV system is presented in Fig. 5 C. The curve fit presented in Fig. 5 C is a log-Gaussian distribution function, and Table 1 shows the different functions that were used and the values of t_d found with each one. The RMS reached with the log-Gaussian function was 0.65%. This result is better than those obtained with the two systems that contain silica beads, because of the higher signal-to-noise ratio obtained for these experi-
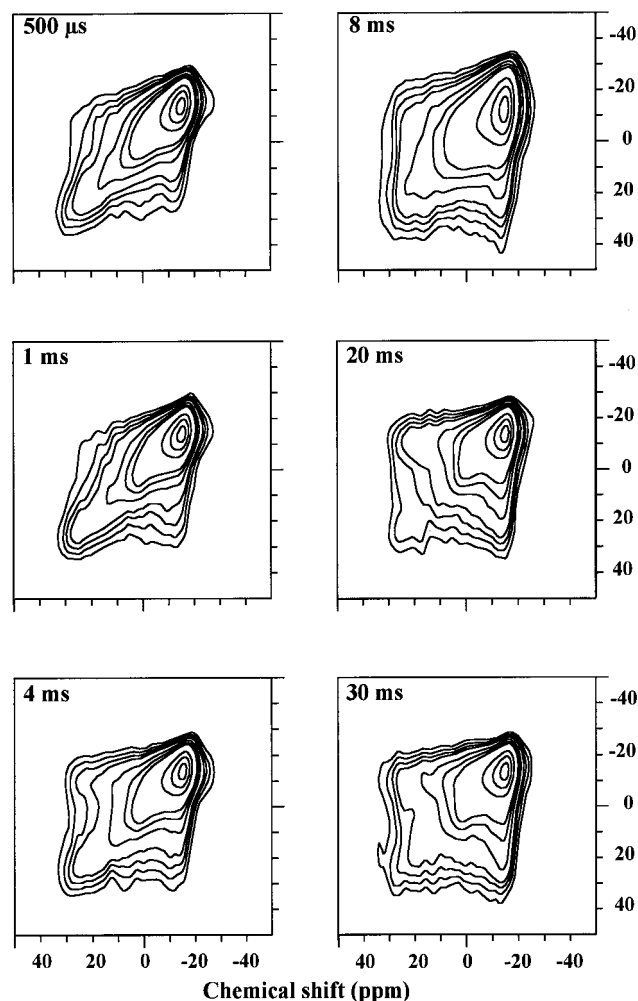
FIGURE 4 2D ^{31}P NMR experimental spectra of pure DPPC MLV at 50°C for different t_m.

FIGURE 5 C_2 as a function of mixing time for (*A*) pure DPPC SSV fitted with a single exponential function, (*B*) SSV of the melittin-DPPC complex fitted with a log-Gaussian distribution, and (*C*) DPPC MLV fitted with a log-Gaussian distribution function.

mental spectra. The KWW function also gives a good RMS value, as expected. The Gaussian distribution function was again discarded, because of the lack of physical significance of the result. The t_d value is greater than those obtained for the two other systems and ranges from 2.8 to 9.3 ms for the log-Gaussian distribution. If we supposed a fixed radius of 0.5 μm (Larsen et al., 1987), a lateral diffusion constant ranging from 5×10^{-8} to 15×10^{-8} cm^2/s would be found. These distributions are presented in Fig. 6, *A* and *B*. The mean values of the lateral diffusion constant for the SSV and MLV preparations are therefore approximately the same if the assumption that a correct value of the MLV radius was used. Of course, avoiding this approximation was the main motivation in using the silica beads. However, if we make the approximation that the mean lateral diffusion constant is the same with and without the beads, we can come back to the radius distribution for the MLV system. This was done using Eq. 13, and the results are presented in Fig. 6 *C*. These results indicate that the radius ranges from 180 to 1300 nm for the MLV system.
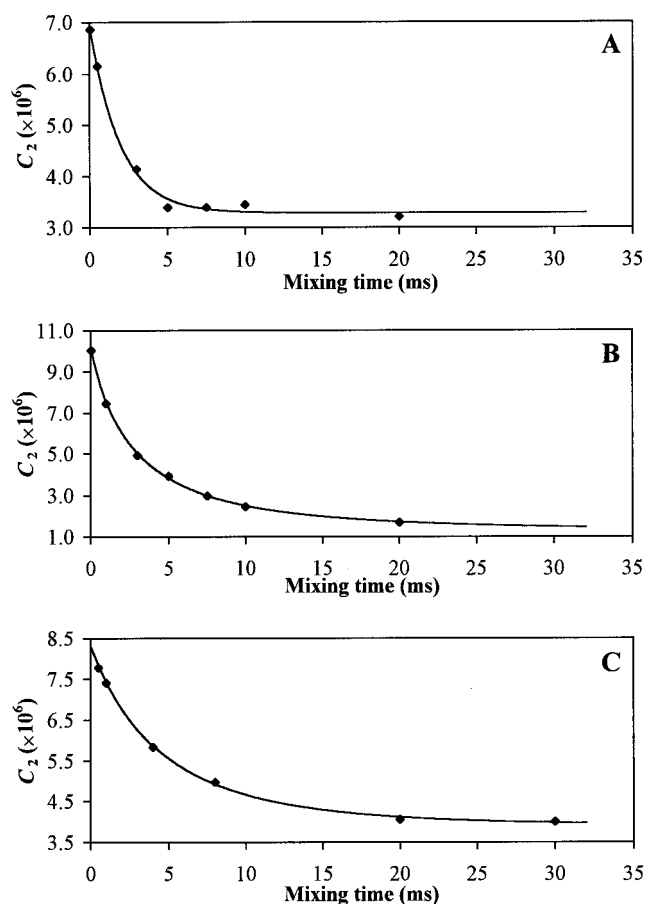
DISCUSSION

Two-dimensional ^{31}P NMR as a tool for the determination of the lateral diffusion constant

Lateral diffusion is a largely studied property of lipids (Vaz et al., 1984; Tocanne et al., 1989). Among the lipids studied, DPPC is certainly the one that has attracted the greatest interest, mainly because of its high transition temperature (41°C), which allows its study in both the liquid crystalline and gel phases. The main technique used to measure the lateral diffusion constant is FRAP, even though this method requires fluorescent probes in concentrations up to 1%. With this technique, diffusion constants from 8×10^{-8} cm^2/s for unilamellar vesicles of DPPC at 50°C (Tamm and McConnell, 1985) up to 13×10^{-8} cm^2/s at 45°C for multilamellar vesicles of DPPC (Vaz et al., 1985) have been measured. Lateral diffusion constants of many other phosphatidylcholines have also been determined in the range of 5×10^{-8} to 14.5×10^{-8} cm^2/s (Vaz et al., 1985; Merkel et al., 1989; Kapitzka et al., 1984). Our mean value of 8.8×10^{-8} cm^2/s for DPPC at 50°C is therefore very close to those determined by FRAP. In addition, the mean value of
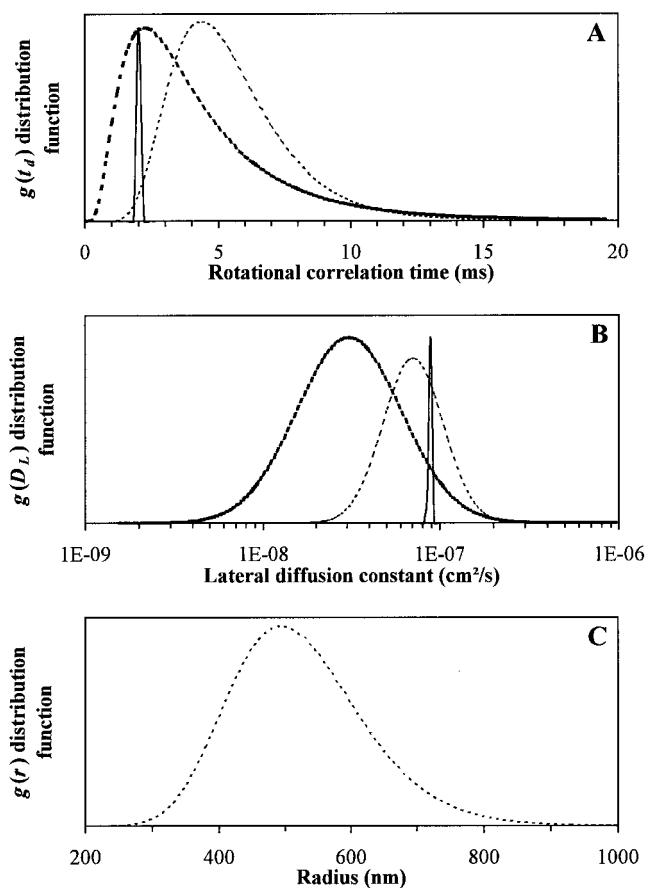
FIGURE 6 (*A*) Distribution of rotational correlation times for DPPC SSV (*solid curve*), DPPC MLV (*light dashed curve*), and melittin-DPPC SSV (*bold dashed curve*). (*B*) Distribution of lateral diffusion constants for DPPC SSV (*solid curve*), DPPC MLV (*light dashed curve*), and melittin-DPPC SSV (*bold dashed curve*). (*C*) Distribution of radii for DPPC MLV.

4.9×10^{-8} cm^2/s determined in the presence of melittin is below the measured values for PCs. Therefore, it appears that melittin effectively slows down the lateral diffusion of DPPC.

Many NMR techniques have also been used for the determination of the lateral diffusion constant of lipids. Among them, there are methods based on the analysis of proton rotating frame longitudinal relaxation times (Lee et al., 1995), of ^{31}P lineshape (Cullis, 1976; Larsen et al., 1987), of deuterium transversal relaxation time measurements (Köchy and Bayerl, 1993), and of deuterium (Dolainsky et al., 1995) and ^{31}P (Fenske and Jarrell, 1991; Fenske et al., 1991) two-dimensional exchange spectra.

Based on ^{31}P lineshape analysis, Cullis (1976) measured a value of 2.6×10^{-8} cm^2/s for the diffusion of DPPC in small unilamellar vesicles, and a constant of 30×10^{-8} cm^2/s was determined by ^{31}P two-dimensional exchange NMR of multilamellar vesicles (Fenske et al., 1991). This two-dimensional method requires the knowledge of the vesicle radius, but the use of multilamellar vesicles always leads to a great approximation of this radius that can be spread up to two orders of magnitude around an average

value (Heaton et al., 1996). The radius of the multilamellar vesicles will also depend greatly on the method of sample preparation. Therefore, the determination of the lateral diffusion constant by two-dimensional NMR methods relies on a precise knowledge or control of the lipid vesicle radius. In addition, if the goal of the study is to determine the effect of a substance (protein, drug) on the lateral diffusion of lipids, one has to be very critical about the results obtained with nonsupported vesicles, because some proteins and drugs can completely reorganize the lipid structures (de Wolf et al., 1991), making it difficult to distinguish between a variation in the lateral diffusion constant and a variation in the radius of the vesicles.

Diffusion measurements have also been performed by the pulse-field gradient (Lindblom and Orädd, 1996) and supercon fringe field gradient (Karakatsanis and Bayerl, 1996) techniques. Despite the fact that these are NMR techniques, the diffusion constants that will be obtained from them should be closer to those obtained by FRAP methods. In practice, the lipids are deposited on glass plates oriented in the magnetic field. The lipids that will undergo diffusion along the gradient (pulsed or static) will be affected by it. Therefore, the lateral diffusion constant will be obtained directly without the need to know the vesicle radii. The quality of the measurement will depend on the quality of the lipid deposit on the glass plates and on the orientation of the glass plates in the NMR magnet. With pulsed-field gradient techniques (PFG), Wennerström and Lindblom (1977) found a value of 12×10^{-8} cm^2/s for DMPC at 50°C. On the other hand, supercon fringe field gradients (SFF), which use the property of the decaying static field outside the homogeneous zone of the magnet, have been used to measure the lateral diffusion constant of DPPC (Karakatsanis and Bayerl, 1996). A value of 14×10^{-8} cm^2/s was found for DPPC at 50°C. However, it is important to mention that this technique requires an additional calibration to characterize the field gradient.

Among the techniques used for the determination of lateral diffusion constants, there is also quasi-elastic neutron scattering (QENS). This technique is particularly sensitive to rapid diffusion, i.e., to diffusion on a time scale of $<10^{-9}$ s and on a distance scale of 2–100 Å. The lateral diffusion constant measured by Tabony and Perly (1990) with this method for DPPC at 63°C is 4×10^{-6} cm^2/s. This constant is two orders of magnitude greater than the ones measured by FRAP and NMR. Because of its time scale, QENS most likely measures a local Brownian motion, whereas NMR and FRAP measure large-scale diffusion (Vaz and Almeida, 1991). Confirmation of these assumptions was given by König et al. (1992), who have measured with QENS for DPPC rapid motions corresponding to diffusion perpendicular and parallel to the bilayer normal ($D^{\perp} = 1.5 \times 10^{-7}$ to 6×10^{-6} cm^2/s and $D^{\parallel} = 2.1 \times 10^{-6}$ cm^2/s), associated with a slow diffusion component ($D_{\mathrm{lat}} = 9.7 \times 10^{-8}$ cm^2/s), corresponding to the lateral diffusion measured by NMR and FRAP. Both the slow and fast diffusion constants can provide helpful information about lipid bilayers. The slow

one is important in the study of lipid-protein interaction and in the study of lateral phase separation, whereas the fast component can be helpful in investigating the effect of protein incorporation in the membrane.

Friction between the bead surface and the phospholipids

An important point that needs to be considered is the friction between the lipid membrane and the solid support, whether the latter is made of silica or germanium, and is planar or spherical. Our results for pure lipids, in comparison with FRAP techniques, tend to demonstrate that this friction is very weak and does not significantly alter the lateral diffusion. In addition, several studies have investigated the effect of the solid substrate on the rate of lipid lateral diffusion (Merkel et al., 1989). The values obtained by the different methods are so close that it seems improbable that the support modifies the diffusion. However, it should be noted that the lipids used in the present study are zwitterionic, and therefore are less likely to interact with the charged solid support compared to charged lipids. On the other hand, systematic studies of the diffusion of lipids on solid supports have shown that the single bilayer directly adsorbed on the surface, i.e., with the highest possible interaction, has the same diffusion constant as the extra bilayers (Merkel et al., 1989). Finally, the gel to liquid-crystalline phase transition temperatures of neutral lipids deposited on solid substrates are modified by only one or two degrees (Bayerl and Bloom, 1990; Naumann et al., 1992). Therefore, we can conclude that the surface does not significantly modify the diffusion of lipids.

The melittin-DPPC-beads system

The results obtained in the present study indicate a decrease and broadening of the distribution of lateral diffusion constants for DPPC in the presence of melittin. Melittin therefore seems to act as an obstacle to the lipid diffusion. Obviously, it is possible that melittin could adsorb directly to the silica beads and become an obstacle to the lipid lateral diffusion, but the fact that small objects unbind from the system at the phase transition temperature (vide supra) suggests that at least some of the melittin molecules are near the bilayer surface.

This is in agreement with previous results suggesting that at 50°C in DPPC, melittin would act as a wedge and disorder the lipid chains (Dufourc et al., 1986b). It has also been reported that melittin would generate lateral defects in the membrane (Dempsey, 1990; Pott and Dufourc, 1995; Pott et al., 1996). One may then imagine that the presence of melittin in the bilayer hinders the lateral diffusion of lipids. Interestingly, it was reported that melittin weakly modifies high-frequency motions (10^9 Hz) (Dufourc et al., 1986b). We demonstrated herein that like other proteins (Bloom and Smith, 1985), melittin also affects low-frequency motions.

Another interesting fact observed in the present study is the quasi-inhibition of the formation of discoidal melittin-DPPC complexes in the gel phase. The presence of small complexes gives rise to an isotropic peak in both ^{31}P and ^{2}H solid-state NMR spectra (Dufourc et al., 1986a,b), so it is usually impossible to study the interaction more deeply by these methods. Therefore, the stabilization of the DPPC-melittin complex on the beads offers a way to study the interaction between melittin and DPPC in the gel phase. For example, it should be possible to study the order of the different deuterons along the lipid acyl chains by ^{2}H solid-state NMR.

CONCLUSION

The present study indicates that the lateral diffusion constant of lipids on radius-controlled supported vesicles can be determined precisely by ^{31}P solid-state 2D NMR. A method, based on the calculation of the autocorrelation time function, was used to determine with great precision the diffusion time t_d and possibly to detect a distribution of diffusion times. For pure DPPC, a diffusion constant in agreement with the ones determined by other techniques has been obtained. In addition, the lateral diffusion of lipids with and without beads is centered around the same value of lateral diffusion constant. The results also show that melittin slows down the lateral diffusion of DPPC and significantly broadens the distribution of lateral diffusion constants. Finally, the melittin-DPPC complex is stabilized at the surface of the silica beads, opening the way to new studies on the complex that were not possible until now, because of the formation of small discoidal structures.

REFERENCES

Abragam, A. 1961. Principle of Nuclear Magnetism. Oxford University Press, London.

Auger, M., and H. C. Jarrell. 1990. Elucidation of slow motion in glyco-glycerolipid bilayers by two-dimensional solid-state deuteron NMR. *Chem. Phys. Lett.* 165:162–167.

Auger, M., I. C. P. Smith, and H. C. Jarrell. 1991. Slow motions in lipid bilayers: direct detection by two-dimensional solid-state deuterium nuclear magnetic resonance. *Biophys. J.* 59:31–38.

Barrall, G. A., K. Schmidt-Rohr, Y. K. Lee, K. Landfester, H. Zimmermann, G. C. Chingas, and A. Pines. 1995. Rotational diffusion measurements of suspended colloidal particles using two-dimensional exchange nuclear magnetic resonance. *J. Chem. Phys.* 104:509–520.

Bayerl, T. M., and M. Bloom. 1990. Physical properties of single phospholipid bilayers adsorbed to microglass beads: a new vesicular model system studied by ^{2}H-nuclear magnetic resonance. *Biophys. J.* 58:357–362.

Bloom, M., and T. M. Bayerl. 1995. Membranes studied using neutron scattering and NMR. *Can. J. Phys.* 73:687–696.

Bloom, M., and I. C. P. Smith. 1985. Manifestation of lipid-protein interactions in deuterium NMR. *In* Progress in Protein-Lipid Interactions. A. Watts and J. J. H. H. M. De Pont, editors. Elsevier/North Holland, Amsterdam, 61–88.

Bloom, M., and E. Sternin. 1987. Transverse nuclear spin relaxation in phospholipid bilayer membranes. *Biochemistry.* 26:2101–2105.

Bodenhausen, G., H. Kogler, and R. R. Ernst. 1984. Selection of coherence-transfer pathways in NMR pulse experiments. *J. Magn. Reson.* 58:370–388.

Brumm, T., A. Möps, C. Dolainsky, S. Brückner, and T. M. Bayerl. 1992. Macroscopic orientation effects in broadline NMR-spectra of model membranes at high magnetic field strength: a method preventing such effects. *Biophys. J.* 61:1018–1024.

Carr, H. Y., and E. Purcell. 1954. Effects of diffusion on free precession in nuclear magnetic resonance experiments. *Phys. Rev.* 94:630–638.

Cornut, I., E. Thiaudière, and J. Dufourcq. 1993. The amphipathic helix in cytotoxic peptides. *In* The Amphipathic Helix. R. P. Epand, editor. CRC Press, Boca Raton, FL. 173–219.

Cullis, P. R. 1976. Lateral diffusion rates of phosphatidylcholine in vesicle membranes: effects of cholesterol and hydrocarbon phase transitions. *FEBS Lett.* 70:223–228.

Dasseux, J. L., J. F. Faucon, M. Lafleur, M. Pézolet, and J. Dufourcq. 1984. A restatement of melittin-induced effects on the thermotropism of zwitterionic phospholipids. *Biochim. Biophys. Acta.* 775:37–50.

Davis, J. H. 1983. The description of membrane lipid conformation, order and dynamics by ^{2}H-NMR. *Biochim. Biophys. Acta.* 737:117–171.

Davis, J. H. 1991. Deuterium nuclear magnetic resonance spectroscopy in partially ordered systems. *In* Isotopes in the Physical and Biomedical Sciences. Elsevier Science Publishers B. V., Amsterdam. 99–157.

Dempsey, C. E. 1990. The actions of melittin on membranes. *Biochim. Biophys. Acta.* 1031:143–161.

Désormeaux, A., G. Laroche, P. E. Bougis, and M. Pézolet. 1992. Characterization by infrared spectroscopy of the interaction of a cardiotoxin with phosphatidic acid and with binary mixtures of phosphatidic acid and phosphatidylcholine. *Biochemistry.* 31:12173–12182.

de Wolf, F. A., M. Maliepaard, F. van Dorsten, I. Berghuis, K. Nicolay, and B. de Kruijff. 1991. Comparable interactions of doxorubicin with various acidic phospholipids results in changes of lipid order and dynamics. *Biochim. Biophys. Acta.* 1096:67–80.

Dolainsky, C., A. Möps, and T. M. Bayerl. 1993. Transverse relaxation in supported and non-supported phospholipid model membranes and the influence of ultraslow motions: a ^{31}P-NMR study. *J. Chem. Phys.* 98:1712–1720.

Dolainsky, C., M. Unger, M. Bloom, and T. M. Bayerl. 1995. Two-dimensional exchange ^{2}H NMR experiments of phospholipid bilayers on a spherical solid support. *Phys. Rev. E.* 51:4743–4750.

Dufourc, E. J., J. M. Bonmatin, and J. Dufourcq. 1989. Membrane structure and dynamics by ^{2}H- and ^{31}P-NMR. Effects of amphipatic peptidic toxins on phospholipid and biological membranes. *Biochimie.* 71:117–123.

Dufourc, E. J., J. F. Faucon, G. Fourche, J. Dufourcq, T. Gulik-Grzywicki, and M. le Maire. 1986a. Reversible disc-to-vesicle transition of melittin-DPPC complexes triggered by the phospholipid acyl chain melting. *FEBS Lett.* 201:205–209.

Dufourc, E. J., I. C. P. Smith, and J. Dufourcq. 1986b. Molecular details of melittin-induced lysis of phospholipid membranes as revealed by deuterium and phosphorus NMR. *Biochemistry.* 25:6448–6455.

Dufourcq, J., J. F. Faucon, G. Fourche, J. L. Dasseux, M. le Maire, and T. Gulik-Grzywicki. 1986. Morphological changes of phosphatidylcholine bilayers induced by melittin: vesicularization, fusion, discoidal particles. *Biochim. Biophys. Acta.* 859:33–48.

Faucon, J. F., J. M. Bonmatin, J. Dufourcq, and E. J. Dufourc. 1995. Acyl chain length dependence in the stability of melittin-phosphatidylcholine complexes. A light scattering and ^{31}P-NMR study. *Biochim. Biophys. Acta.* 1234:235–243.

Fenske, D. B., and P. R. Cullis. 1992. Chemical exchange between lamellar and non-lamellar lipid phases. A one- and two-dimensional ^{31}P-NMR study. *Biochim. Biophys. Acta.* 1108:201–209.

Fenske, D. B., and H. C. Jarrell. 1991. Phosphorus-31 two-dimensional solid-state NMR: application to model membrane and biological systems. *Biophys. J.* 59:55–69.

Fenske, D. B., M. Letellier, R. Roy, I. C. P. Smith, and H. C. Jarrell. 1991. Effects of calcium on the dynamic behavior of sialylglycerolipids and phospholipids in mixed model membranes. A ^{2}H and ^{31}P NMR study. *Biochemistry.* 30:10542–10550.

Fringeli, U. P., and H. H. Günthard. 1981. Infrared membrane spectroscopy. *In* Membrane Spectroscopy. E. Grell, editor. Springer Verlag, New York. 270–332.

Griffin, R. G. 1981. Solid state nuclear magnetic resonance of lipid bilayers. *Methods Enzymol.* 72:108–174.

Heaton, J. H., G. Althoff, and G. Kothe. 1996. Observation of lateral diffusion in biomembranes by excitation transfer ^{31}P NMR: estimation of vesicle size distribution. *J. Phys. Chem.* 100:4944–4953.

Jeener, J., B. H. Meier, P. Bachmann, and R. R. Ernst. 1979. Investigation of exchange processes by two-dimensional NMR spectroscopy. *J. Chem. Phys.* 71:4546–4553.

Johnson, S. J., T. M. Bayerl, D. C. McDermott, G. W. Adam, A. R. Rennie, R. K. Thomas, and E. Sackmann. 1991. Structure of an adsorbed dimyristoyl phosphatidylcholine bilayer measured with specular reflection of neutrons. *Biophys. J.* 59:289–294.

Kapitzka, H. G., D. A. Rüppel, H. J. Galla, and E. Sackmann. 1984. Lateral diffusion of lipids and glycophorin in solid phosphatidylcholine bilayers: the role of structural defects. *Biophys. J.* 45:577–587.

Karakatsanis, P., and T. M. Bayerl. 1996. Diffusion measurements in oriented phospholipid bilayers by ^{1}H-NMR in a static fringe field gradient. *Phys. Rev. E.* 54:1785–1790.

Katsu, T., M. Kuroko, T. Morikawa, K. Sanchika, Y. Fujita, H. Yamamura, and M. Uda. 1989. Mechanism of membrane damage induced by the amphipathic peptides gramicidin S and melittin. *Biochim. Biophys. Acta.* 983:135–183.

Katsu, T., C. Ninomiya, M. Kuroko, H. Kobayashi, T. Hirota, and Y. Fujita. 1988. Action of amphipathic peptides gramicidin S and melittin on erythrocyte membrane. *Biochim. Biophys. Acta.* 939:57–63.

Köchy, T., and T. M. Bayerl. 1993. Lateral diffusion coefficients of phospholipids in spherical bilayers on a solid supported measured by ^{2}H-nuclear magnetic resonance relaxation. *Phys. Rev. E.* 47:2109–2116.

König, S., W. Pfeiffer, T. Bayerl, D. Richter, and E. Sackmann. 1992. Molecular dynamics of lipid bilayers studied by incoherent quasi-elastic neutron scattering. *J. Phys. II (France).* 2:1589–1615.

Larsen, D. W., J. G. Boylan, and B. Cole. 1987. Axially symmetric ^{31}P NMR line shapes with selective excitation in the presence of lateral diffusion on a curved surface. *J. Phys. Chem.* 91:5631–5634.

Lee, B. S., S. A. Mabry, A. Jonas, and J. Jonas. 1995. High-pressure proton NMR study of lateral self-diffusion of phosphatidylcholines in sonicated unilamellar vesicles. *Chem. Phys. Lipids.* 78:103–117.

Lindblom, G., and G. Orädd. 1996. Liquid-crystalline samples: diffusion. *In* Encyclopedia of Nuclear Magnetic Resonance. John Wiley, Chichester, England. 2760–2768.

Lis, L. J., M. McAlister, N. Fuller, and R. P. Rand. 1982. Interactions between neutral phospholipid bilayer membranes. *Biophys. J.* 37:657–665.

Macquaire, F., and M. Bloom. 1995. Membrane curvature studied using two-dimensional NMR in fluid lipid bilayers. *Phys. Rev. E.* 51:4735–4742.

Meiboom, S., and D. Gill. 1958. Modified spin-echo method for measuring nuclear relaxation times. *Rev. Sci. Instrum.* 29:688–691.

Merkel, R., E. Sackmann, and E. Evans. 1989. Molecular friction and epitactic coupling between monolayers in supported bilayers. *J. Phys. France.* 50:1535–1555.

Nabet, A., J. M. Boggs, and M. Pézolet. 1994. Study by infrared spectroscopy of the interaction of bovine myelin basic protein with phosphatidic acid. *Biochemistry.* 33:14792–14799.

Naumann, C., T. Brumm, and T. M. Bayerl. 1992. Phase transition behavior of single phosphatidylcholine bilayers on a solid spherical support studied by DSC, NMR and FT-IR. *Biophys. J.* 63:1314–1319.

Pott, T., and E. J. Dufourc. 1995. Action of melittin on the DPPC-cholesterol liquid-ordered phase: a solid-state ^{2}H- and ^{31}P-NMR study. *Biophys. J.* 68:965–977.

Pott, T., J. Dufourcq, and E. J. Dufourc. 1996. Fluid to gel phase lipid bilayers to study peptide membrane interactions? *Eur. Biophys. J. Biophys. Lett.* 25:55–59.

Rance, M., and R. A. Byrd. 1983. Obtaining high-fidelity spin ½ powder spectra in anisotropic media: phase-cycled Hahn echo spectroscopy. *J. Magn. Reson.* 52:221–240.

Reinl, H. M., and T. M. Bayerl. 1993. Interaction of myelin basic protein with single bilayers on a solid support: an NMR, DSC and polarized infrared ATR study. *Biochim. Biophys. Acta.* 1151:127–136.

Schaefer, D., and H. W. Spiess. 1992. Two-dimensional exchange nuclear magnetic resonance of powder samples. IV. Distribution of correlation times and line shapes in the intermediate dynamic range. *J. Chem. Phys.* 97:7944–7954.

Schmidt-Rohr, K., and H. W. Spiess. 1994. Multidimensional Solid-State NMR and Polymers. Academic Press, London.

Seelig, J. 1977. Deuterium magnetic resonance: theory and applications to lipid membranes. *Q. Rev. Biophys.* 10:353–418.

Seelig, J. 1978. ^{31}P nuclear magnetic resonance and the head group structure of phospholipids in membranes. *Biochim. Biophys. Acta.* 515:105–140.

Singer, S. J., and G. L. Nicolson. 1972. The fluid mosaic model of the structure of cell membranes. *Nature.* 175:720–731.

Smith, I. C. P., and I. H. Ekiel. 1984. Phosphorus-31 NMR of phospholipids in membranes. *In* Phosphorus-31 NMR: Principles and Applications. D. Gorenstein, editor. Academic Press, London. Ch. 15. 447–475.

Spiess, H. W. 1991. 2D NMR: elucidation of molecular dynamics in complex systems. *J. Non-Cryst. Solids.* 131–133:766–772.

Tabony, J., and B. Perly. 1990. Quasielastic neutron scattering measurements of fast local translational diffusion of lipid molecules in phospholipid bilayers. *Biochim. Biophys. Acta.* 1063:67–72.

Tamm, L. K., and H. M. McConnell. 1985. Supported phospholipid bilayers. *Biophys. J.* 47:105–113.

Tocanne, J. F., L. Dupou-Cézanne, A. Lopez, and J. F. Fournier. 1989. Lipid lateral diffusion and membrane organization. *FEBS Lett.* 257:10–16.

Vaz, W. L. C., and P. F. Almeida. 1991. Microscopic versus macroscopic diffusion in one-component fluid phase lipid bilayer membranes. *Biophys. J.* 60:1553–1554.

Vaz, W. L. C., R. M. Clegg, and D. Hallmann. 1985. Translational diffusion of lipids in liquid crystalline phase phosphatidylcholine multibilayers: a comparison of experiment with theory. *Biochemistry.* 24:781–785.

Vaz, W. L. C., F. Goodsaid-Zalduondo, and K. Jacobson. 1984. Lateral diffusion of lipids and proteins in bilayer membranes. *FEBS Lett.* 174:199–207.

Wennerström, H., and G. Lindblom. 1977. Biological and model membranes studied by nuclear magnetic resonance of spin one half nuclei. *Q. Rev. Biophys.* 10:67–96.

Williams, G., and D. C. Watts. 1970. Nonsymmetrical dielectric relaxation from a simple decay function. *Trans. Faraday Soc.* 66:80–85.